Front. Phys., 2014, 9(2): 200–209
DOI 10.1007/s11467-013-0409-6

RESEARCH ARTICLE

Effects of various defects on the electronic properties of single-walled carbon nanotubes: A first principle study

Qing-Xiao Zhou[1,2], **Chao-Yang Wang**[2], **Zhi-Bing Fu**[2], **Yong-Jian Tang**[2], **Hong Zhang**[1,3,†]

[1] *College of Physical Science and Technology, Sichuan University, Chengdu 610065, China*
[2] *Research Center of Laser Fusion, China Academy of Engineering Physics, Mianyang 621900, China*
[3] *Key Laboratory of High Energy Density Physics and Technology of Ministry of Education, Sichuan University, Chengdu 610064, China*
Corresponding author. E-mail: †*hongzhang@scu.edu.cn*
Received July 5, 2013; accepted December 8, 2013

The geometries, formation energies and electronic band structures of (8, 0) and (14, 0) single-walled carbon nanotubes (SWCNTs) with various defects, including vacancy, Stone–Wales defect, and octagon–pentagon pair defect, have been investigated within the framework of the density-functional theory (DFT), and the influence of the concentration within the same style of defect on the physical and chemical properties of SWCNTs is also studied. The results suggest that the existence of vacancy and octagon–pentagon pair defect both reduce the band gap, whereas the SW-defect induces a band gap opening in CNTs. More interestingly, the band gaps of (8, 0) and (14, 0) SWCNTs configurations with two octagon–pentagon pair defect presents 0.517 eV and 0.163 eV, which are a little smaller than the perfect CNTs. Furthermore, with the concentration of defects increasing, there is a decreasing of band gap making the two types of SWCNTs change from a semiconductor to a metallic conductor.

Keywords carbon nanotube, density functional theory, defect, electronic structure

PACS numbers 31.15.Ew, 61.72.Bb

1 Introduction

Carbon based nanostructure materials, carbon nanotubes and graphene, are considered as the most favorable candidates for many future technological applications because of their unique properties [1–4]. Nevertheless, carbon nanotubes usually suffer from various types of topological defect during their growth. A great amount of experiments and theory has demonstrated that the existence of defects [5, 6], such as vacancies [7], Stone–Wales (SW) defect [8], Octagon–pentagon pair defect [9], inverse Stone–Wales (ISW) defect [10], pentagon–heptagon pair defect [11] in the carbon nanostructures produce a significant influence on the mechanical [12] and electronic properties [13, 14], exhibiting to be useful for achieving some desired functionalities [15–17]. Defect sites of vacancies present higher reactivity for adsorption, which makes chemical fictionalization an easy method to detect imperfections on CNTs and graphene. Orellana studied the interaction of H_2 molecules and CNTs with multivacancy defects using molecular dynamic simulations and the binding energies were found to be 0.14–0.21 eV/H_2 at room temperature [18]. Nishidate *et al.* applied the density-function theory to investigate the lithium ion adsorption on SWCNTs with vacancies, and the results suggest that the possibility of accumulation of lithium ions inside the SWCNTs with large defective rings [19]. SW-defect acts as a typical topological defect consisting of two pairs of five-member and seven-member rings. Choi *et al.* reported that SW-defects can reduce or close the band gap in large band gap CNTs, but increase it in metallic CNTs [20]. Lee *et al.* found that a vacancy hole reconstructed into two separated pentagon-heptagon pair defects which is preceded by the subsequent Stone–Wales [21]. Qin *et al.* found that the graphene with SW defect is more sensitive than that of perfect graphene for detecting H_2CO molecules [22]. The octagon–pentagon pair defect is a common defect during the growth of carbon nanotubes, which shows that C-C bond lengths and angles are reasonable for sp^2 hybridization. A one-dimension defect consisting of one octagon and a pair of pentagon periodically repeated alone the dislocation line in CNTs exhibits magnetic ordering

[16]. Yang *et al.* presented a study of chromium-chain-embedded carbon nanotubes with a line defect consisting of octagon–pentagon pair defects. They found that the configuration exhibits a local spin band gap and acts as a quasi-one-dimensional half–metallic mechanism [17]. All the results above suggest that the presence of defects dramatically affect the properties of CNTs.

In this paper, we focus on three types of defect, namely, vacancy, Stone–Wales defect, and octagon-pentagon pair defect, reducing or increasing the band gap of the semiconductor (8, 0) and (14, 0) SWCNTs by using density-functional theory (DFT) calculations. Furthermore, geometry structures, formation energies and frontier molecular orbitals are also investigated for the same style of defect with various concentrations.

2 Computational details and model constructing

All the calculations are performed with the framework of first-principles DFT approach implemented in the Dmol^3 package [22]. The exchange-correlation interaction and functional are treated within the generalized gradient approximation (GGA) and Perdew–Burke–Ernzerhof (PBE) function. Double numerical basis set with polarization functions (DNP) is selected and the DFT semi-core pseudopotential (DSSP) is used for the relativistic effects, which replaces core electron by a single effective potential [23]. In order to obtain the ground geometries of nanotubes, the conjugate-gradient minimization schemes are utilized. The optimization will continue, until the energy fluctuation is less than 2×10^{-5} Ha and the force on each atom are not greater than 0.002 Ha/Å. Monkhorst–Pack special k-points of $1\times1\times6$ meshes are used to represent the Brillouin zone for all structures. The global orbital cutoff is set to be 5.0 Å. To accelerate the electron convergence, the value of smearing of 0.002 Ha is used. In this report we use (8, 0) and (14, 0) zig-zag SWCNT, which are common semiconductors, as representative models to investigate the effect of three different styles of defect and various number on the geometries and electronic structures of different diameter SWCNTs. As shown in Figs. 1(a) and (b), a hexagonal supercell is adopted, whose size are $20.00 \times 20.00 \times 8.52$ Å^3, with the length of c in the axial of z direction being two times of the periodicity of the (8, 0) and (14, 0) nanotubes, respectively. The nearest distance between neighboring nanotubes is more than 20.00 Å, and the interaction between neighboring nanotubes images could be neglected.

The gaps between highest occupied molecular orbital (HOMO) and lowest unoccupied molecular orbital (LUMO) of the modified structures are calculated in this study. The chemical activity of CNTs can be characterized by the HOMO-LOMO energy gap that is a significant parameter relying on the HOMO-LOMO energy levels. Typically, a small HOMO-LOMO energy gap means a high chemical activity and a low stability. The corresponding calculations of HOMO-LOMO gaps are at the Gamma point. Moreover, in defected systems, the key physical quantity to calculate is the defect formation energy which many properties of a defect can be obtained from variations and in vacancy system it is defined as

$$E_{\mathrm{f}} = E_{\mathrm{d}} - m\mu_{\mathrm{C}} \tag{1}$$

where E_{d} is the total energy of the defect SWCNT, the chemical potential of μ_{C} is the energy per carbon atom in the optimized perfect SWCNT, and the m is the number of carbon atoms in defect SWCNT. The formation energies for Stone–Wales and octagon–pentagon pair defects are defined as

$$E_{\mathrm{f}} = (E_{\mathrm{d}} - m\mu_{\mathrm{C}})/n \tag{2}$$

in Eq. (2), n is the number of defects, the others are same as Eq. (1). Typically, we concern $n = 1, 2, 3, 4$ in the present work.

3 Results and discussion

3.1 vacancy defects

Firstly, we optimized the perfect SWCNTs and calculated their electronic band structures (Fig. 1). The valence band maximum and the conduction band minimum are both located at F symmetry point with the band gap of 0.626 eV and 0.354 eV for (8, 0) and (14,0) SWCNT, which well agrees with 0.620 eV and 0.390 eV reported in the previous literature [24, 25].

For the vacancy in nanotubes, we consider single-vacancy (SV), double-vacancy (DV), treble-vacancy (TV), and fourfold-vacancy (FV) defects. The DV, TV and FV structures may miss atom towards different orientations, and in our study we foucus on the adjacent C atoms near the missing atom in SV configuration. After full relaxation, there are geometry distortions in all these structures, which is more exquisite with the quantity of vacancies increasing (Fig. 2). The perfect carbon nanotubes has a stable structure with sp^2-bonding and π-bonding perpendicular p_z-orbitals, but the appearance of vacancies induce some valence electrons and bond with other carbon atoms. The formation energies imply the stabilization of configurations with defect and that of

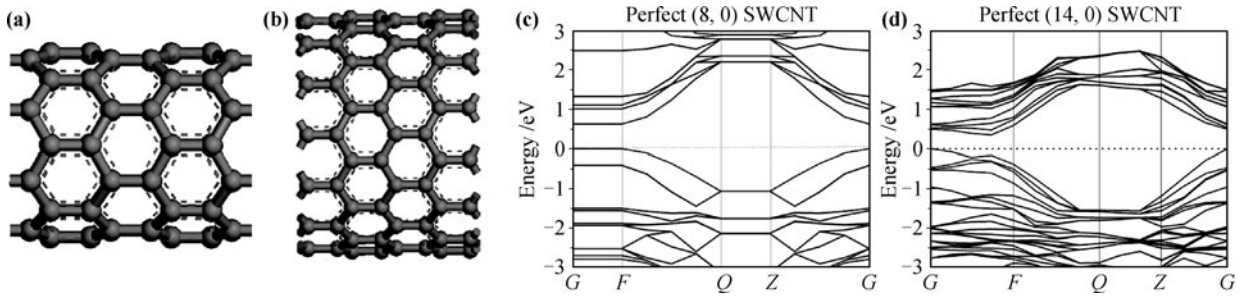

Fig. 1 Optimized geometries of (8, 0) **(a)** and (14, 0) **(b)** SWCNTs; the electronic band structures of (8, 0) **(c)** and (14, 0) **(d)** SWCNTs.

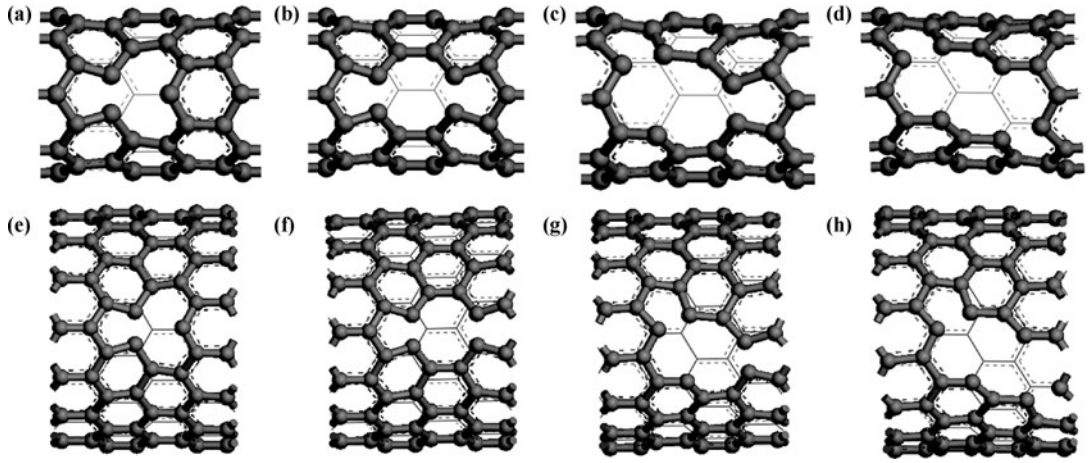

Fig. 2 Optimized geometries of (8, 0) and (14, 0) SWCNTs with single-vacancy (SV) **(a, e)**, double-vacancy (DV) **(b, f)**, treble-vacancy (TV) **(c, g)**, and fourfold-vacancy (FV) **(d, h)**.

vacancies defined in Eq. (1) are listed in Table 1. It can be learned that the FV has the highest formation energy in the two types of defected SWCNTs system, which results from the most existence of the dangling bond of carbon atom than others. From this reason, the SV and TV are definitely lower than fourfold-vacancies. Nevertheless, the DV acts as the lowest owing to the structure come into being a pair of octagon-pentagon defect, which owns good symmetry and exhibits better stability [Figs. 2(b) and (e)]. Moreover, the formation energies of the same number vacancy, the (14, 0) SWCNT exhibits a little larger than that of (8, 0) SWCNT. This difference can be explained by the curvature effect, as shown in previous investigations [26].

The gaps of HOMO-LOMO for the perfect and defected SWCNTs are shown in Fig. 3, which are changing with the number of vacancy defect increasing. For the perfect (8, 0) and (14, 0) SWCNTs, the gaps are all largest than other defected systems. This indicates the perfect structure is stable, but the presence of vacancy induces the decreasing of HOMO-LOMO gap and the system with most vacancies presents the lowest gap and most unstable. The V-2 configuration in two types of SWCNT owns the largest HOMO-LOMO gap, which is in accord with the results of lowest formation energies. That indicates the appearance of octagon-pentagon defect on account of double vacancy in SWCNT and it is consistent with the former discussion.

Table 1 Calculated formation energies (E_f) and band gap (E_g) of (8, 0) and (14, 0) SWCNTs with vacancy-style defects: single-vacancy (SV), double-vacancy (DV), treble-vacancy (TV), and fourfold-vacancy (FV) defects.

Energy	(8, 0) SWCNT				(14, 0) SWCNT			
	V-1	V-2	V-3	V-4	V-1	V-2	V-3	V-4
E_f /eV	5.381	3.709	7.924	13.171	5.984	4.106	8.630	13.238
E_g /eV	0.381	0.054	0.027	0	0.027	0.052	0	0.026

In the case of SV defect in (8, 0) SWCNT [Fig. 4(a)], it is found that dangling bonds associated with the vacancy introduced localized empty defect states between the conduction band and valence band, which is similar to (14, 0) SWCNT shown in Fig. 4(e). Moreover, the degeneracy associated with the top energy levels in valence band of the perfect SWCNT is lifted and the dispersion of these levels is also reduced, which suggests that these states are becoming more localized. For the (8, 0) SWCNT, the value of band gap is narrowed by 0.245 eV compared with the perfect nanotubes. For other

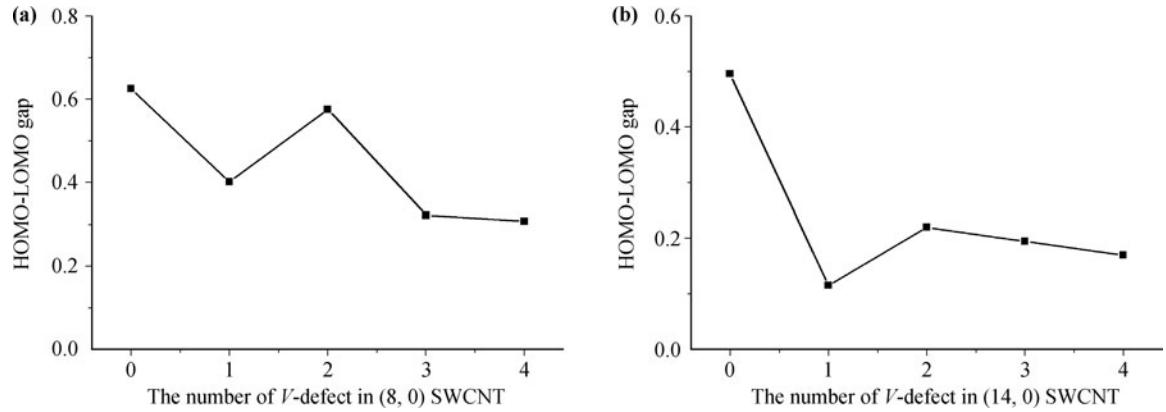

Fig. 3 The variety of HOMO-LOMO gaps with the number of vacancy defect (V-defect) increasing in (8, 0) SWCNT **(a)** and (14, 0) SWCNT **(b)**.

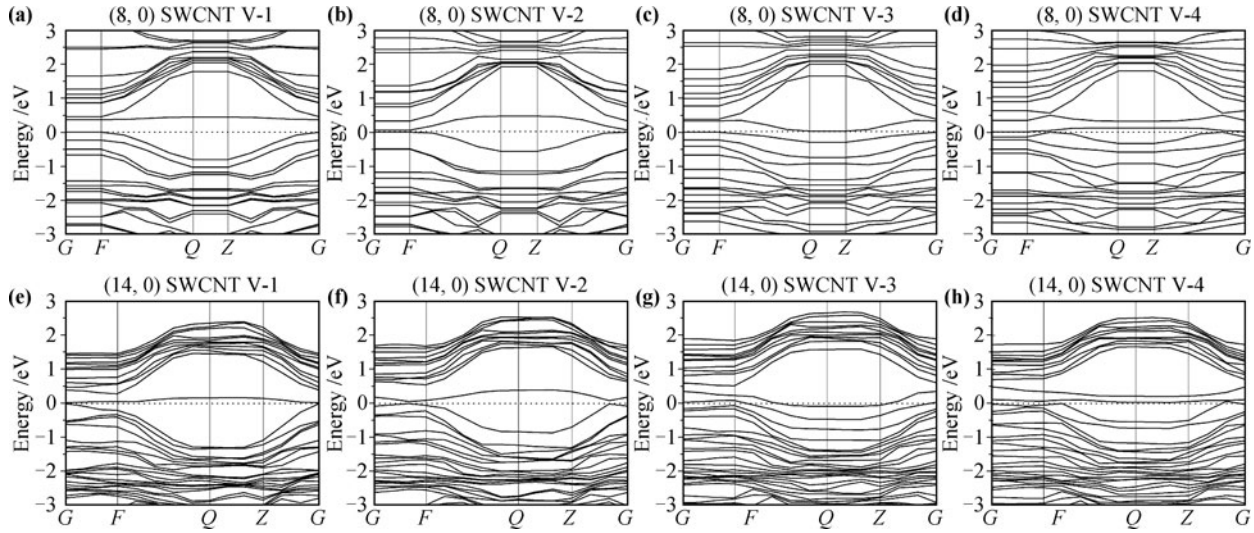

Fig. 4 The electronic band structures of (8, 0) and (14, 0) SWCNTs with single-vacancy (SV) **(a, e)**, double-vacancy (DV) **(b, f)**, treble-vacancy (TV) **(c, g)**, and fourfold-vacancy (FV) **(d, h)**.

cases of (8, 0) defected SWCNT, they are similar to the case of SV, and the value of energy gap is reducing with the numbers of vacancies increasing (Table 1). Especially for the FV structure, the configuration changes from a direct-gap semiconductor into a metallic conductor. In (14, 0) SWCNT configurations, the band gap is also decreasing owning to the presence of vacancy. Meanwhile, the value of band gap for DV structure is 0.052 eV, which is the largest than other three configurations, and the TV structure exhibit metallic. Then, we can learn that the existence of vacancy produces a band gap reducing for different diameter semiconductor of zig-zag SWCNTs.

3.2 Stone–Wales defects

Stone–Wales defect significantly influences on the mechanical and electronic properties of CNTs. We consider four configurations with SW-defects ranging from one to four, represented by SW-1, SW-2, SW-3, and SW-4. The multi-defects structure constructed along the circle of SWCNT are taken into account. Figure 5 shows the optimized structures. The defect atoms move out of the wall towards the opposite direction for lower energy by allowing the compressed carbon bonds in its contiguity to expand. Furthermore, the structures of SW-2 and SW-4 present geometry symmetry. From Fig. 5, we can learn that the distortion of (8, 0) is more obvious than (14, 0) SWCNT. It is because of the (14, 0) owns larger diameter and then has a relative lower defect concentration. The corresponding formation energies are listed in Table 2, which clearly illuminate that the formation energies increase with the number of SW-defects increasing for (8, 0) and (14, 0) CNTs. In addition, single-particle theory of defect formation energy calculation shows that there are both attraction and repulsion between SW-defects and the most energetically favorable arrangement is setting them just next to each other but not overlapping [27, 28]. In Fig. 6, the variety of HOMO-LOMO

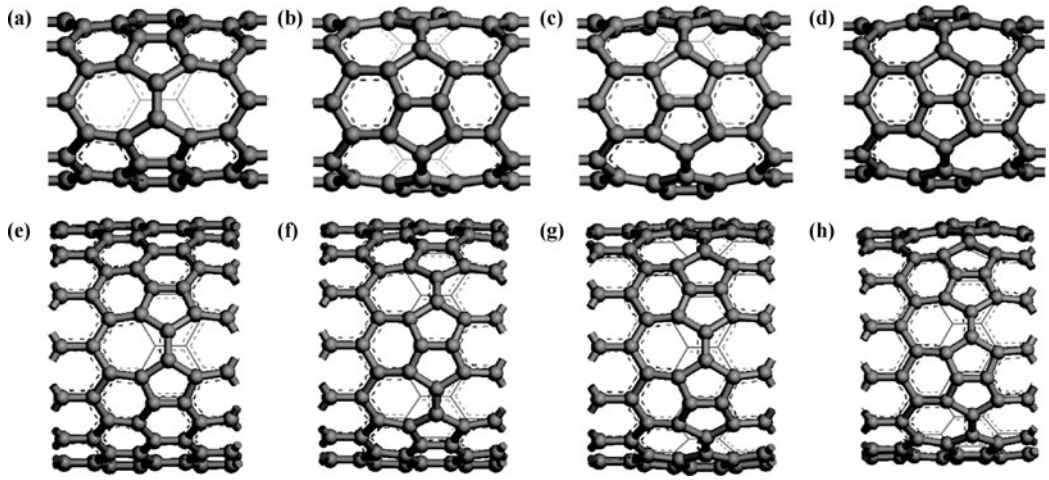

Fig. 5 Optimized geometries of (8, 0) and (14, 0) SWCNTs with SW-1 **(a, e)**, SW-2 **(b, f)**, SW-3 **(c, g)**, and SW-4 **(d, h)**.

gaps is illustrated for all the structures with different number of SW-defects. For (8, 0) SWCNT with a SW-defect, it manifests higher value than perfect one, which maybe result from the 18-electrons rule forming in SW defect. Whereas the number of SW-defect is augment, the gaps are becoming lower and lower, which makes out the structure owns worse stabilization.

Table 2 Calculated formation energies (E_f) and band gap (E_g) of (8, 0) and (14, 0) CNT with SW-style defects.

Energy	(8, 0) SWCNT				(14, 0) SWCNT			
	SW-1	SW-2	SW-3	SW-4	SW-1	SW-2	SW-3	SW-4
E_f /eV	3.083	3.447	3.570	3.821	4.325	4.812	5.057	5.232
E_g /eV	0.789	0.653	0.218	0.216	0.399	0.327	0.027	0

SW-defects remarkably influence the electronic properties by introducing defect states into the band gap region. The band structures and the band gap of (8, 0) and (14, 0) SWCNTs with different quantities of SW-defects are shown in Fig. 7 and Table 2, respectively. We first analyzed the (8, 0) SWCNT. In Fig. 7(a), the minimum level of valence band is lifted at F point, aggrandizing the energy gap with one SW-defect. This is because the quantity of electron in the nanotubes with the SW-defect is deficient compared with the perfect nanotubes. The band gaps of the SW-1 and SW-2 are 0.789 eV and 0.653 eV, and they both are greater than 0.626 eV of the perfect CNT, which is caused by the broken of π bond by introducing SW-defects. These results suggest that the carbon atoms near SW-defect region has more charge transfer, which changes the band gap at sites close to and far from the SW-defect region. These phenomena have been found experimentally [29, 30]. Whereas, the band gaps of SW-3 and SW-4 are smaller than the perfect, which agree with the theory that the stabilization is becoming lower because of the more defect destroying the stable structure in perfect CNTs. In the case of (14, 0) defected SWCNT, it is similar to the (8, 0) SWCNT. The value of band gap for SW-1 is 0.399 eV, which is a little larger than perfect (14, 0) SWCNT with the value of 0.354 eV. With the number of SW-defect increasing, the SW-4 configuration change to a conductor. Therefore, we can be obtained that the presence of

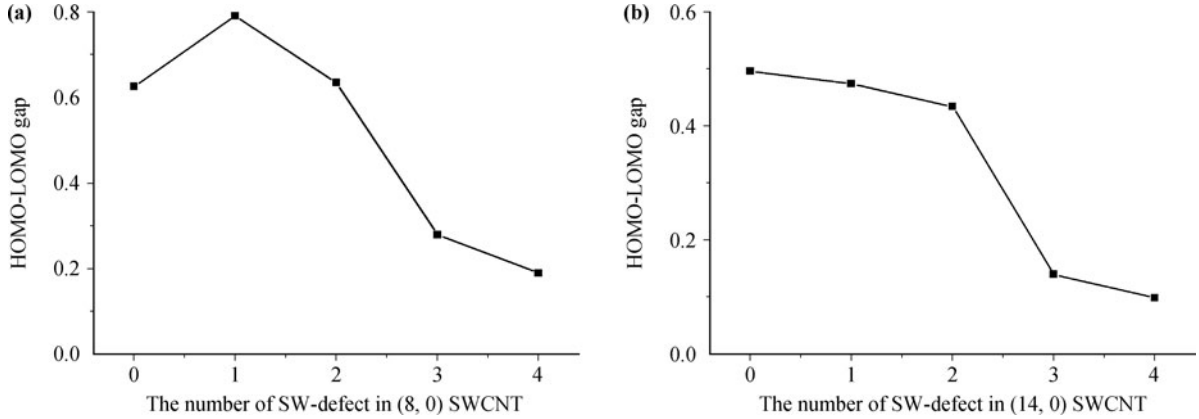

Fig. 6 The variety of HOMO-LOMO gap with the number of Stone–Wales defect (SW-defect) increasing in (8, 0) **(a)** SWCNT and (14, 0) SWCNT **(b)**.

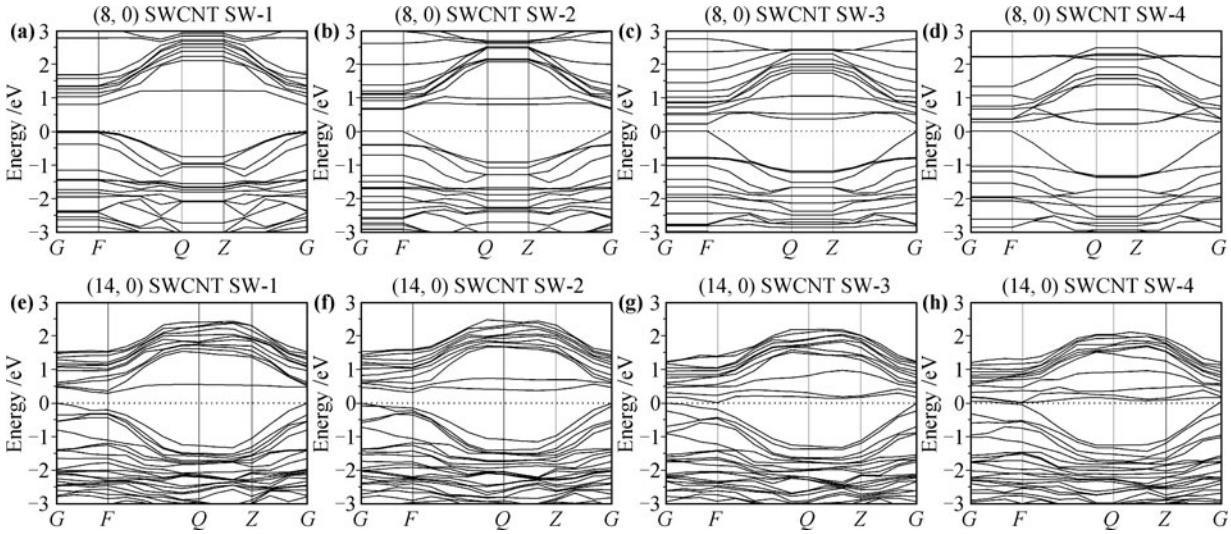

Fig. 7 The electronic band structures of (8, 0) and (14, 0) SWCNTs with SW-1 **(a, e)**, SW-2 **(b, f)**, SW-3 **(c, g)**, and SW-4 **(d, h)**.

Stone–Wales defect enlarges the band gap of (8, 0) and (14, 0) SWCNTs and the value is decreasing with the quantities of SW-defect increasing. Moreover, the formation energies are becoming large which indicate the stabilization of configurations is becoming worse.

3.3 Octagon-pentagon pair defects

In this part, we also consider four configurations which have diverse numbers of octagon-pentagon pair defect, namely, OP-1, OP-2, OP-3, and OP-4. The multi-defects configurations are built along the wall encircling CNTs, which is similar to SW-defect structures. The optimized defected configurations of (8, 0) and (14, 0) SWCNTs are depicted in Fig. 8, which presents some distortion in all structures. The carbon atoms composing the octagon–pentagon pair defect are depressed toward the center axis of nanotubes in order to stabilize the stretched and compressed C-C bonds. Interestingly, the OP-4 of (8, 0) SWCNTs having four OP-style defects presents consummate symmetry. For (8, 0) SWCNTs structures, the formation energies are reducing with the number of octagon–pentagon pair defects increasing as illustrated in Table 3, which is contrary to the SW-defects. The decrement of formation energy of OP-style defects in (8, 0) SWCNT can be explained by the much better geometry symmetry stabilizing the structure. By contraries, the more OP-style defects in (14, 0) SWCNTs, the larger formation energies are. That suggests that the configuration is more instable with the presence of octagon–pentagon pair defects. The difference between the (8, 0) and (14, 0) SWCNTs may be resulted from the curvature effect due to the different diameter. Furthermore, the HOMO-LOMO gaps (Fig. 9) substantiate above results.

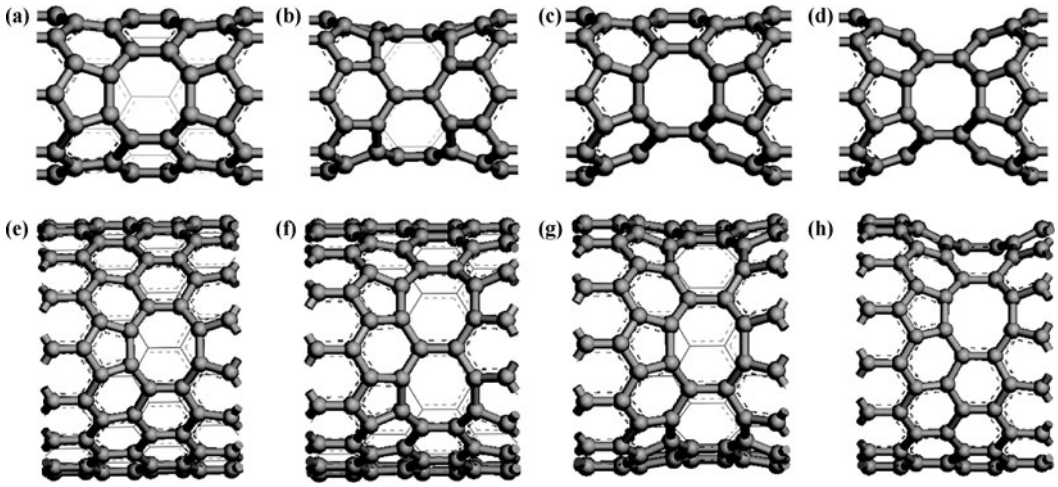

Fig. 8 Optimized geometries of (8, 0) and (14, 0) SWCNTs with octagon–pentagon pair defects: OP-1 **(a, e)**, OP-2 **(b, f)**, OP-3 **(c, g)**, and OP-4 **(d, h)**.

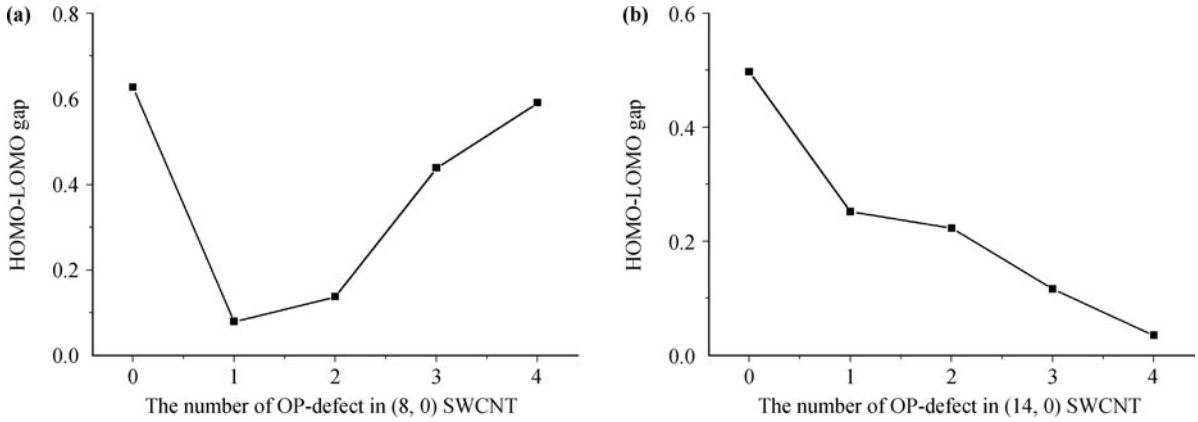

Fig. 9 The variety of HOMO-LOMO gap with the number of octagon–pentagon pair defect (OP-defect) increasing in (8, 0) SWCNT **(a)** and (14, 0) SWCNT **(b)**.

Table 3 Calculated formation energies (E_f) and band gap (E_g) of (8, 0) and (14, 0) SWCNTs with octagon–pentagon pair defects.

Energy	(8, 0) SWCNT				(14, 0) SWCNT			
	OP-1	OP-2	OP-3	OP-4	OP-1	OP-2	OP-3	OP-4
E_f /eV	3.684	3.367	3.260	2.959	4.102	4.230	4.398	4.466
E_g /eV	0.054	0.517	0	0	0.054	0.163	0	0

To further understand the effect of octagon–pentagon pair defects on the electric properties, the band structures are calculated (Fig. 10). As well as the behavior of vacancy defect, the semiconductor (8, 0) and (14, 0) SWCNTs transform into a metallic conductor by introducing OP-style defect. We take (8, 0) SWCNT as example. In Fig. 10(a), the presence of defect gives rise to descend of the flat band of valence band and the lifting of conduction band near the Fermi level. As for the Figs. 10(c) and (d), the flat bands overlap through the Fermi level illustrating the metallic of CNTs. Noteworthy, the OP-2 of (8, 0) SWCNT [Fig. 10(b)] presents 0.517 eV of band gap, it is a little smaller than perfect CNT. Moreover, the OP-2 of (14, 0) SWCNT exhibits 0.163 eV, which is twice times small than that of perfect (14, 0) SWCNT. To explore the reason, we performed the local density of states (LDOS) of carbon atoms composing an octagon–pentagon pair defect of (8, 0) SWCNT (Fig. 8).

In CNTs, p_x and p_y orbital of carbon atoms interact to form σ and σ^* bonds in plane. Meanwhile, the p_z orbital combined create π and π^* bonds and the π bond is perpendicular to the plane which σ bonds are in. The hybridization of σ and π at sites surrounding the octagon–pentagon pair defect influence the local density of states, especially in conductance band area. We performed the DOS of carbon atoms at defect sites of the OP-defected CNTs and the perfect one. For OP-1, the DOS peak near the Fermi level disappears and splits into two flat peaks below and above the Fermi level. In OP-2, the two peaks around the Fermi level are much stronger than OP-1 and the strength are similar with that of perfect

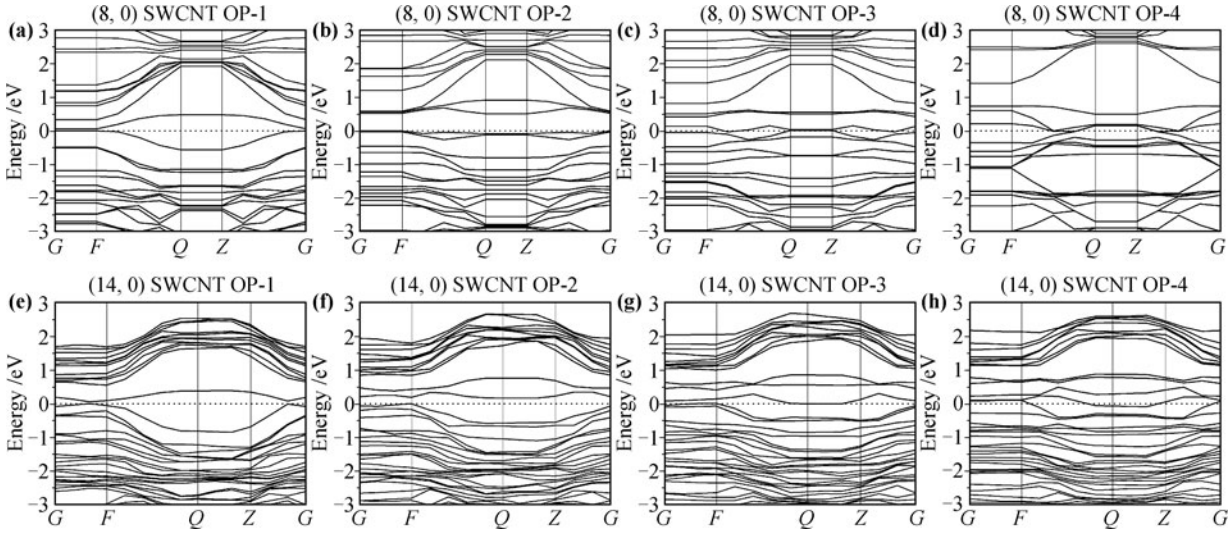

Fig. 10 The electronic band structures of (8, 0) and (14, 0) SWCNTs with octagon–pentagon pair defects: OP-1 **(a, e)**, OP-2 **(b, f)**, OP-3 **(c, g)**, and OP-4 **(d, h)**.

(8, 0) CNTs. In the case of OP-3, the DOS peaks around the Fermi level are flat and ranging through the Fermi level. As to OP-4, a sharp peak at the Fermi level appears and results to the structure changes to conductivity. Then we can learn that the carbon atoms forming the defect of OP-1, OP-3, and OP-4 [Figs. 11(b), (d), (e)] have more charge transfer in conductance near Fermi level compared with OP-2. This indicates that the OP-2

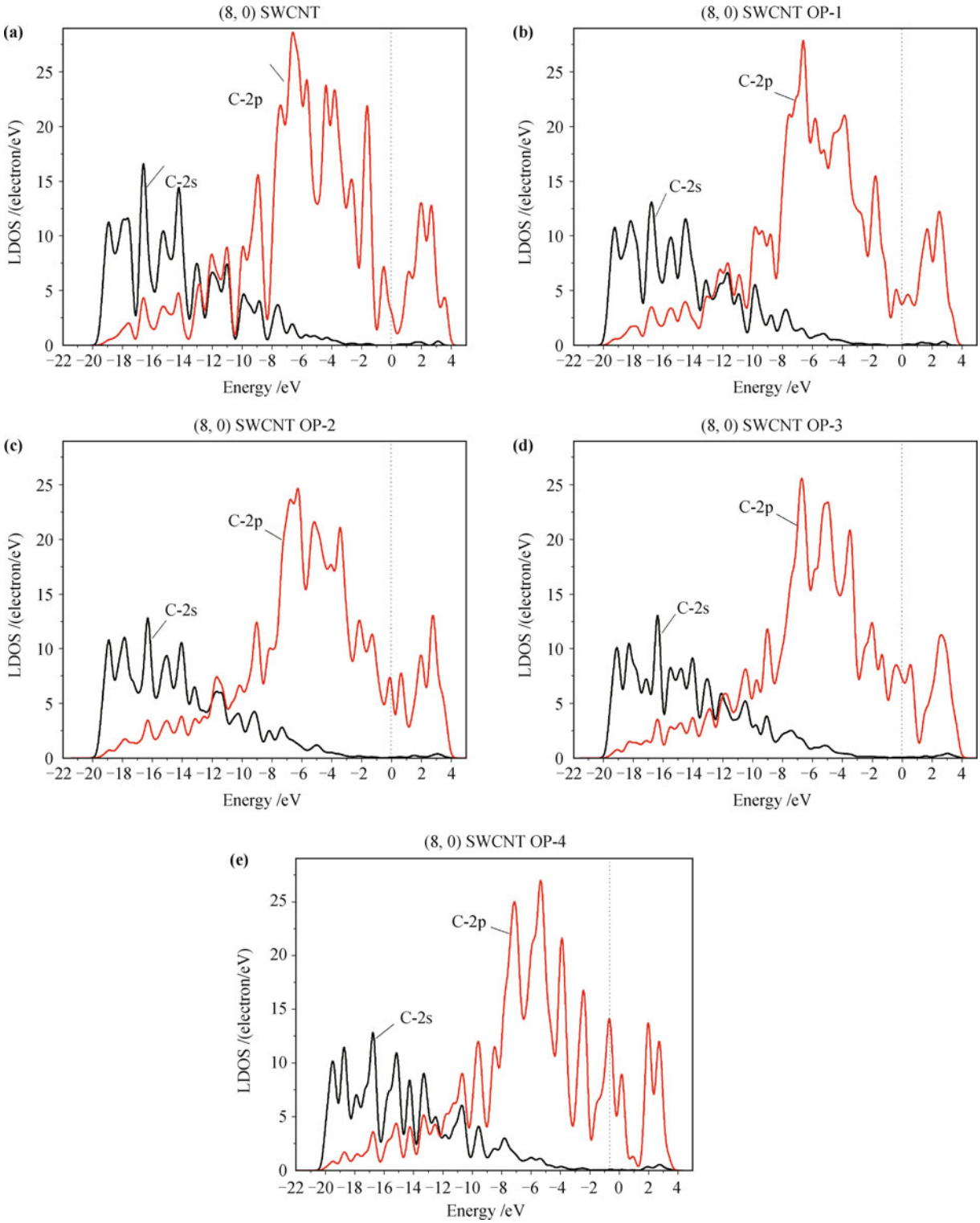

Fig. 11 The LDOS of p orbital of carbon atoms composing an octagon–pentagon pair defect in defected (8, 0) SWCNTs: **(a)** Perfect (8, 0) SWCNTs, **(b)** OP-1, **(c)** OP-2, **(d)** OP-3, and **(e)** OP-4.

configuration has less local states of electron resulting in a band gap of 0.517 eV. However, the formation energies of OP-style defect in (8, 0) SWCNT is becoming small with the quantities of defect increasing, which is contrary to that of (14, 0) SWCNT. The band structures are changed by introducing the OP-defect, which reduces the value of band gap making the (8, 0) and (14, 0) defected SWCNTs transform into metallic conductors.

4 Conclusion

We have investigated the geometries and electronic structures of (8, 0) and (14, 0) carbon nanotubes with various styles of defect by using the first-principles total-energy calculation in the density-function theory. Our results imply that the formation energies of defect in (8, 0) SWCNT are increasing with the concentration rising of vacancy and SW-defect, but the configuration having octagon-pentagon pair defect is decreasing. This is because the OP-defect in (8, 0) SWCNT presents excellent geometry symmetry to stable the configurations. As to the configurations of (14, 0) defected SWCNT, the formation energies of three types of defect are increasing with the increase of qualities of defects. Simultaneously, for these two types of SWCNTs with different diameter, the vacancies induce a decreasing of band gap, and with the number of vacancies increasing the CNT transforms into a metallic conductor. The similar exhibition owns by the case of octagon–pentagon pair defects too, but the OP-2 structures of (8, 0) and (14, 0) SWCNTs are distinct from the other three configurations. Especially, the band gap of OP-2 of (8, 0) SWCNT is 0.517 eV and it is a little smaller than the perfect (8, 0) SWCNTs. We can learn from the LDOS of OP-defected (8, 0) SWCNT that these noticeable phenomena are resulted from the less charge transfer in conductance band near the Fermi level of OP-2 than that of OP-1, OP-3, and OP-4 do. Whereas, there is a band gap opening in the case of SW-defect for both (8, 0) and (14, 0) SWCNTs, because of the broken the π bond of carbon atoms and induces the localized electronic states as defect emergence. It is expected that the above results could ultimately foster the applications of CNTs and open field for research in the future.

Acknowledgements This work was supported by the National Natural Science Foundation of China (Grant Nos. 11074176, 10976019 and 51101141), the Research Fund for the Doctoral Program of Higher Education of China (Grant No. 20100181110080), and the Research Found from Science and Technology on Plasma Physics Laboratory (Grant No. 9140C680502C68254).

References

1. R. Martel, T. Schmidt, H. R. Shea, T. Hertel, and P. Avouris, Single- and multi-wall carbon nanotube field-effect transistors, *Appl. Phys. Lett.*, 1998, 73(17): 2447
2. Y. W. Son, M. L. Cohen, and S. G. Louie, Electric field effects on spin transport in defective metallic carbon nanotubes, *Nano Lett.*, 2007, 7(11): 3518
3. Z. W. Zhang, J. C. Li, and Q. Jiang, Density functional theory calculations of the metal-doped carbon nanostructures as hydrogen storage systems under electric fields: A review, *Front. Phys.*, 2011, 6(2): 162
4. L. F. Huang and Z. Zheng, Patterning graphene nanostripes in substrate-supported functionalized graphene: A promising route to integrated, robust, and superior transistors, *Front. Phys.*, 2012, 7(3): 324
5. H. Zhu, K. Suenaga, A. Hashimoto, K. Urita, and S. Iijima, Structural identification of single and double-walled carbon nanotubes by high-resolution transmission electron microscopy, *Chem. Phys. Lett.*, 2005, 412(1–3): 116
6. M. Ouyang, Energy gaps in "metallic" single-walled carbon nanotubes, *Science*, 2001, 292(5517): 702
7. J. Huang, S. Chen, Z. Ren, Z. Wang, K. Kempa, M. Naughton, G. Chen, and M. Dresselhaus, Enhanced ductile behavior of tensile-elongated individual double-walled and triple-walled carbon nanotubes at high temperatures, *Phys. Rev. Lett.*, 2007, 98(18): 185501
8. A. J. Stone and D. J. Wales, Theoretical studies of icosahedral C_{60} and some related species, *Chem. Phys. Lett.*, 1986, 128(5–6): 501
9. J. Lahiri, Y. Lin, P. Bozkurt, I. I. Oleynik, and M. Batzill, An extended defect in graphene as a metallic wire, *Nat. Nanotechnol.*, 2010, 53: 1
10. M. T. Lusk, D. T. Wu, and L. D. Carr, Graphene nanoengineering and the inverse-Stone–Thrower–Wales defect, *Phys. Rev. B*, 2010, 81(15): 155444
11. G. D. Lee, C. Z. Wang, E. Yoon, N. M. Hwang, and K. M. Ho, The role of pentagon–heptagon pair defect in carbon nanotube: The center of vacancy reconstruction, *Appl. Phys. Lett.*, 2010, 97(9): 093106
12. A. V. Krasheninnikov and K. Nordlund, Ion and electron irradiation-induced effects in nanostructured materials, *J. Appl. Phys.*, 2010, 107(7): 071301
13. A. Tolvanen, G. Buchs, P. Ruffieux, P. Gröning, O. Gröning, and A. Krasheninnikov, Modifying the electronic structure of semiconducting single-walled carbon nanotubes by Ar^+ ion irradiation, *Phys. Rev. B*, 2009, 79(12): 125430
14. C. X. Zhang, C. He, Z. Yu, L. Xue, K. W. Zhang, L. Z. Sun, and J. Zhong, Effects of oxygen-containing defect complex on the electronic structures and transport properties of single-walled carbon nanotubes, *Phys. Lett. A*, 2012, 376(20): 1686

15. M. Bockrath, Resonant electron scattering by defects in single-walled carbon nanotubes, *Science*, 2001, 291(5502): 283

16. S. Okada, K. Nakada, K. Kuwabara, K. Daigoku, and T. Kawai, Ferromagnetic spin ordering on carbon nanotubes with topological line defects, *Phys. Rev. B*, 2006, 74(12): 121412

17. Y. Yang, Y. Xiao, W. Ren, X. Yan, and F. Pan, Half-metallic chromium-chain-embedded wire in graphene and carbon nanotubes, *Phys. Rev. B*, 2011, 84(19): 195447

18. W. Orellana, Reaction and incorporation of H_2 molecules inside single-wall carbon nanotubes through multivacancy defects, *Phys. Rev. B*, 2009, 80(7): 075421

19. K. Nishidate and M. Hasegawa, Energetics of lithium ion adsorption on defective carbon nanotubes, *Phys. Rev. B*, 2005, 71(24): 245418

20. H. Choi, J. Ihm, S. G. Louie, and M. L. Cohen, Defects, quasibound states, and quantum conductance in metallic carbon nanotubes, *Phys. Rev. Lett.*, 2000, 84(13): 2917

21. G. D. Lee, C. Z. Wang, E. Yoon, N. M. Hwang, and K. M. Ho, The formation of pentagon-heptagon pair defect by the reconstruction of vacancy defects in carbon nanotube, *Appl. Phys. Lett.*, 2008, 92(4): 043104

22. X. Qin, Q. Y. Meng, and W. Zhao, Effects of Stone–Wales defect upon adsorption of formaldehyde on graphene sheet with or without Al dopant: A first principle study, *Surf. Sci.*, 2011, 605(9–10): 930

23. J. P. Perdew, K. Burke, and M. Ernzerhof, Generalized gradient approximation made simple, *Phys. Rev. Lett.*, 1996, 77(18): 3865

24. B. Delley, From molecules to solids with the DMol^3 approach, *J. Chem. Phys.*, 2000, 113(18): 7756

25. P. J. F. Harris, Carbon Nanotubes and Related Structures: New Materials for the Twenty-First Century, Cambridge: University of Ontario Press, 1999

26. E. Durgun, S. Dag, V. Bagci, O. Gülseren, T. Yildirim, and S. Ciraci, Systematic study of adsorption of single atoms on a carbon nanotube, *Phys. Rev. B*, 2003, 67(20): 201401

27. X. Blase, L. X. Benedict, E. L. Shirley, and S. G. Louie, Hybridization effects and metallicity in small radius carbon nanotubes, *Phys. Rev. Lett.*, 1994, 72(12): 1878

28. B. I. Yakobson, G. Samsonidze, and G. G. Samsonidze, Atomistic theory of mechanical relaxation in fullerene nanotubes, *Carbon*, 2000, 38(11–12): 1675

29. G. G. Samsonidze, G. G. Samsonidze, and B. I. Yakobson, Energetics of Stone–Wales defects in deformations of monoatomic hexagonal layers, *Comput. Mater. Sci.*, 2002, 23(1–4): 62

30. D. Tekleab, D. Carroll, G. Samsonidze, and B. Yakobson, Strain-induced electronic property heterogeneity of a carbon nanotube, *Phys. Rev. B*, 2001, 64(3): 035419